662–668 Nucleic Acids Research, 1994, Vol. 22, No. 4

Intracellular oligonucleotide hybridization detected by fluorescence resonance energy transfer (FRET)

S.Sixou, F.C.Szoka Jr, G.A.Green, B.Giusti[1], G.Zon[1] and D.J.Chin[2,*]
School of Pharmacy, University of California, San Francisco, CA 94143-0446, [1]Lynx Therapeutics Inc., 465 Lincoln Centre Drive, Foster City, CA 94404 and [2]The Agouron Institute, 505 Coast Blvd, La Jolla, CA 92037, USA

Received August 25, 1993; Revised and Accepted December 31, 1993

ABSTRACT

Fluorescence resonance energy transfer (FRET) was used to study hybrid formation and dissociation after microinjection of oligonucleotides (ODNs) into living cells. A 28-mer phosphodiester ODN (+PD) was synthesized and labeled with a 3′ rhodamine (+PD-R). The complementary, antisense 5′-fluorescein labeled phosphorothioate ODN (−PT-F) was specifically quenched by addition of the +PD-R. In solution, the −PT-F/+PD-R hybrid had a denaturation temperature of 65 ± 3°C detected by both absorbance and FRET. Hybridization between the ODNs occurred within 1 minute at 17 μM and was not appreciably affected by the presence of non-specific DNA. The pre-formed hybrid slowly dissociated ($T_{1/2} \approx 3$ h) in the presence of a 300-fold excess of the unlabeled complementary ODN and could be degraded by DNAse I. Upon microinjection into the cytoplasm of cells, pre-formed fluorescent hybrids dissociated with a half-time of 15 minutes, which is attributed to the degradation of the phosphodiester. Formation of the hybrid from sequentially injected ODNs was detected by FRET transiently in the cytoplasm and later in the cell nucleus, where nearly all injected ODNs accumulate. This suggests that antisense ODNs can hybridize to an intracellular target, of exogenous origin in these studies, in both the cytoplasm and the nucleus.

INTRODUCTION

Synthetic antisense ODNs have been proposed as therapeutic agents to treat viral infections or metastatic diseases (1, 2). This form of therapy is predicated on the formation of a hybrid between the antisense molecule and the message or gene sequence. In numerous studies, hybridization between the target and antisense molecule in cells has been inferred from either the loss of a specific function or from specific protein inhibition (3). In a lesser number of studies a decrease in message levels has been documented (4, 5). However only in oocytes has a message fragment, consistent with an RNAse H mediated degradation of an antisense-message duplex, been identified (6). Not surprisingly, there have been no reports on the detection of a hybrid between conjugate pairs in living cells.

There has, however, been a number of groups that have used fluorescence resonance energy transfer (FRET) to detect the formation of hybrids between ODNs in solution (7–9). The formats for these studies have involved short complementary sequences where the labels were positioned on the 5′ end (7, 9) as well as complementary sequences where one strand contained a donor fluorophore on the 5′ end and the complementary strand was labeled with an appropriate acceptor on the 3′ position (7, 8). These groups have established that fluorescence non-radiative energy transfer can detect ODN hybridization in solution and pointed the way for using this technique in living cells. In this report, we describe for the first time, the use of FRET in living cells to directly study the formation and dissolution of hybrids and their localization by quantitative confocal microscopy.

EXPERIMENTAL PROCEDURES

Oligonucleotides

Three 28-mer *Rev* ODNs were used in these studies. A sense strand phosphodiester ODN spanning the translation initiation region (5′ AGCAGCGAACAGAGGCGAAGAAGGACGG 3′) and an antisense phosphorothioate anti-*Rev* ODN (5′ TCGTCGC-TGTCTCCGCTTCTTCCTGCCA 3′) labeled at the 5′ end with fluorescein (−PT-F), were supplied by Lynx therapeutics Inc. (Foster City, CA). As a control, a 16-mer ODN, complementary to the murine β actin messenger RNA and rhodamine labeled at the 3′ end, was used (Actin-Rho, 5′ GGCGGCCCACG-ATGGA 3′, Lynx therapeutics Inc.). The synthesis and purification of these ODNs were previously described (10). Briefly, an aminohexylphosphate linker spacer at the 5′ or 3′ end was used to attach the fluorescent derivative. The sense strand phosphodiester was also prepared with a 3′-labeled rhodamine (+PD-R). This ODN was synthesized with an amino group attached to the 3′ end *via* a 6-carbon spacer (Synthecell, MD), purified, and labeled with rhodaminetetramethylisothiocyanate in 100 mM Na_2CO_3, pH 9 at room temperature overnight. The reaction was quenched with 3.4 mM NH_4Cl, the samples purified by exclusion column chromatography and electrophoresis in 7.0 M urea to separate the labeled from unlabeled ODN after visualization by UV shadowing. After precipitation and washing

*To whom correspondence should be addressed

in 70% ethanol, the ODNs were resuspended in TE buffer (10 mM Tris−HCl, pH 8 and 1 mM EDTA) and quantified by absorbance at 260 nm (Absorbance units at 260 nm or A units).

Fluorescence measurements

Fluorescence measurements were made in a SPEX Fluorolog 2 spectrophotometer (Spex Industries, Edison, NJ) equipped with a temperature controlled chamber. The excitation wavelength fluorescein was 470 nm and 540 nm for rhodamine. The emission wavelengths used for fluorescein and rhodamine were 522 and 580 nm, respectively. In all experiments the background fluorescence intensity of the phosphate buffer (10 mM phosphate buffer and 100 mM NaCl, pH 7) was negligible in comparison with all the fluorescein or rhodamine derivative samples.

Fluoresence energy transfer characterization. ODNs were mixed in a 2 ml final volume of the phosphate buffer. The control sample was 0.0166 A units/ml (about 0.5 μg/ml, i.e. 17 μM final concentration) of −PT-F (donor compound) without acceptor compound. To this control sample were compared samples containing either the nonlabeled (+PD) or the labeled (+PD-R) acceptor at 1:0.25, 1:1 and 1:4 molar ratios. All the samples were denatured for 20 minutes at 80°C and gradually cooled to room temperature. Emission spectra were recorded, at room temperature, between 500 and 600 nm with excitation at 470 nm. Fluorescein fluorescence quenching (Q) was calculated as follows: $Q = (1-(F_{(donor+acceptor)}/F_{(donor\ alone)}))\times 100$ where F = fluorescence level at 522 nm. The rhodamine fluorescence increase value (I) was computed as $I = (F'_{(donor+acceptor)}/(F'_{(donor\ alone)} + F'_{(acceptor\ alone)}))\times 100$ where F′ = fluorescence level at 580 nm. All the results are expressed as percentages.

Fluorescence and absorbance melting curves. Samples contained the labeled donor (−PT-F) and phosphate buffer only, or nonlabeled (+PD), or labeled (+PD-R) acceptors in 1:1 molar ratios. All samples were denatured as described above and allowed to equilibrate at 10°C. For each sample, the fluorescence intensity at 522 nm was recorded (excitation at 470 nm) while the temperature was slowly increased (at 1°C/minute) with gentle stirring, or the absorbance was measured at 260 nm while the temperature was increased at 0.5°C/minute.

DNase I action. A sample containing the labeled donor and acceptor in a 1:1 ratio (0.0166 A units/ml) in 2 ml of phosphate buffer containing 6 mM $MgCl_2$, was heat denatured as previously described. When the temperature was equilibrated at 37°C, 5 μl of DNase I (10 UI/μl, Boehringer Mannheim, Germany) were added. The excitation and emission wavelengths were 470 nm and 522 nm respectively.

Further characterization: 37°C hybridization, displacement and ssDNA additions. These experiments were performed without heat denaturation. Other experimental conditions were the same as described above (1:1 molar ratios with excitation and emission at 470 and 522 nm respectively). The 3.7 kb ssDNA (a human liver Flavin-containing monooxygenase II cDNA fragment subcloned into Bluescript plasmid KS+) was kindly provided by N.Lomri from the J.Cashman laboratory at UCSF, CA. About 0.5 μg of ssDNA in 2.5 μl of water was added in the 2 ml sample.

Cell culture and microinjection

Mouse (3T3) and African Green Monkey (BSC-1) cell lines were obtained from the American Type Cell Culture collection (Bethesda, MD) and grown in either 10% newborn or fetal calf serum. The cell culture conditions and methods for microinjection of ODNs were previously described (12). Briefly, cells were seeded onto 25 mm diameter coverslips, grown 24−48 hrs and subsequently microinjected with 50−100 fl of ODNs in distilled water or 20 mM Hepes−HCl, pH 7.3, 30 mM KCl at 37°C.

Confocal laser scanning microscopy and image processing

A confocal laser scanning module (Noran Instruments, WI) attached to an inverted microscope (Nikon, NY) was used to monitor fluorescein fluorescence emission (500−540 nm) and rhodamine emission (605−665 nm, Omega, VT). A 60x Plan Apo N.A. 1.4 lens (Nikon, NY) was used for both microinjection and fluorescence. Illumination by the argon laser of the confocal module could be switched amongst band-pass filters for 488, 529, or 474/476 nm excitation lines. Band-pass filters and a secondary dichroic mirror (580 nm) were installed in the confocal module to maximize the specific detection of fluorophore emissions.

To prevent photobleaching, the confocal microscope was operated under conservative conditions (low illumination and intermediate slit positions, 15−25 microns, to maximize signal strength). Changes in donor (−PT-F) fluorescence was not a result of photobleaching since increasing the interval between timepoints (15−30 min) gave similar results.

Custom software was employed to integrate control of the confocal module's functions with a frame-grabbing card (Perceptics, TN) resident within a Macintosh IIfx microcomputer. Images were stored on both hard and optical disk and analyzed by Image v. 1.45 (Wayne Rasband, NIH).

RESULTS

Solution hybridization experiments

Fluorescence transfer characterization. The efficiency of FRET between the donor (−PT-F) and the acceptor (+PD-R) was studied by scanning the emission spectra from 500 to 600 nm

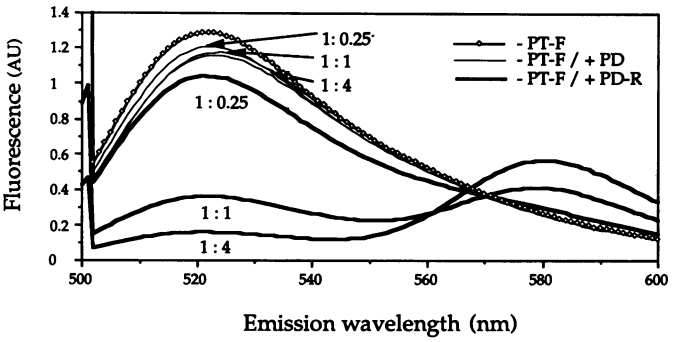

Figure 1. Emission spectra of the donor alone (−PT-F) or mixed with either the non labeled (+PD) or the labeled (+PD-R) acceptor, at different molar ratios. Line A: −PT-F alone, 0.0166 A units/ml ; lines B, C, D respectively: 0.0166 A units/ml plus 0.0208 A units/ml, 0.0833 A units/ml, 0.333 A units/ml of +PD; lines E, F, G respectively: 0.0166 A units/ml plus 0.0041 A units/ml, 0.0166 A units/ml, 0.0666 A units/ml of +PD-R. These correspond in all cases to 1:0.25, 1:1 and 1:4 molar ratios of donor and acceptor.

(maxima for fluorescein and rhodamine were 522 and 580 nm, respectively) at various donor:acceptor molar ratios (1:0.25, 1:1 and 1:4) with labeled (+PD-R) or unlabeled (+PD) acceptors, (Figure 1). With the non-labeled +PD acceptor, the fluorescein emission decreased 8% while the rhodamine emission was unchanged (Figure 1). This phenomenon represents a non-specific quenching of the donor fluorescence in the absence of energy transfer. Hybridization with the labeled acceptor (+PD-R), results in 85.3 ± 1.8% (n=4) donor emission quenching (522 nm) and up to a 70.7 ± 19.6% (n=4) increase in the rhodamine emission (580 nm) that represents the energy transfer. The FRET results of the 1:1 and 1:4 donor:acceptor ratios were also confirmed by life-time measurements (not shown).

Displacement of specific hybridization. The stability of pre-formed hybrid complexes (1:1 molar ratio of either −PT-F/+PD-R or −PT-F/+PD) was studied by the effects of a 300-fold excess of the appropriate acceptor. The +PD-R acceptor was unable to quench more than 10% of the fluorescein emission of a −PT-F/+PD hybrid after 3 hrs (not shown). Similarly, the +PD acceptor showed a 1st order decrease of a −PT-F/+PD-R hybrid's FRET with a $T_{1/2}$ = 3 h (data not shown). These results indicate that the hybrid is stable and the off-rate of the pre-formed complex is quite slow.

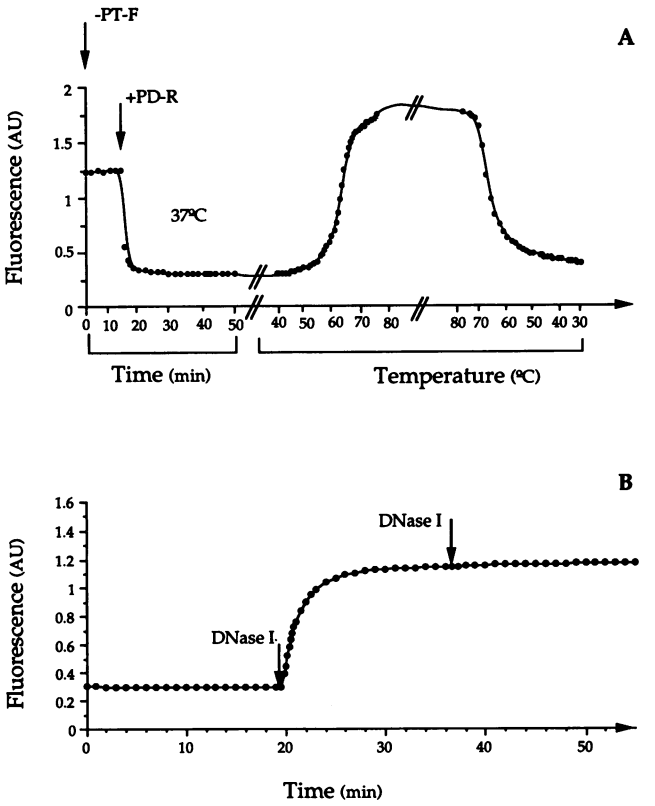

Figure 2. A. Hybridization at 37°C of the donor (−PT-F) with the labeled acceptor (+PD-R), followed by heating and slow cooling of the sample. A 1:1 molar ratio of the ODNs (0.0166 A units/ml each) were mixed and the emission followed for 50 minutes at 37°C whereupon the temperature was progressively raised and lowered. **B.** Degradation at 37°C of the pre-formed hybrid (−PT-F/+PD-R, 1:1 molar ratio, 0.0166 A units/ml each). Two successive additions indicated by the arrows, of DNase I were added (50 UI in a 2 ml sample).

Spontaneous hybridization below the Tm of the hybrid. The Tm of the +PD-R/−PT-F hybrid detected by absorbance and fluorescence was about 65°C in 10 mM phosphate buffer and 100 mM NaCl, pH 7 (not shown). Since fluorescence quenching at 20°C (85%) was maintained at 37°C (83%), we measured the extent of spontaneous hybridization of −PT-F and +PD-R at 37° C. After mixing at 37°C, the fluorescein emission was quenched by 75%. The spontaneous hybridization at 37°C occurs within 1 minute and the extent of hybridization is the same as observed after denaturation and reannealing during progressive cooling (Figure 2A).

Visualization of hybrid degradation. When DNase I is added to the solution containing the hybrid, total recovery of the fluorescein intensity was observed (75% recovery for the 1:1 acceptor:donor molar ratio), (Figure 2B). This result is most simply explained by degradation of the hybrid by the nuclease.

Effect of ssDNA on fluorescence quenching. To approximate the conditions that an ODN might encounter within a cell, we assessed the potential interference of nonspecific nucleic acids on the hybridization reaction. The donor fluorescein-labeled ODN (−PT-F) was first mixed with ssDNA at 37°C, this resulted in a 3.5% non-specific quenching of the fluorescein emission. The labeled acceptor (+PD-R) was subsequently added and the expected quenching (74%) was observed (1:1 molar ratio of acceptor:donor, data not shown).

Microinjection experiments

Since hybridization is robust at near-physiological conditions in the test tube, we microinjected the ODNs into living cells and examined their distribution and hybridization behavior by confocal microscopy.

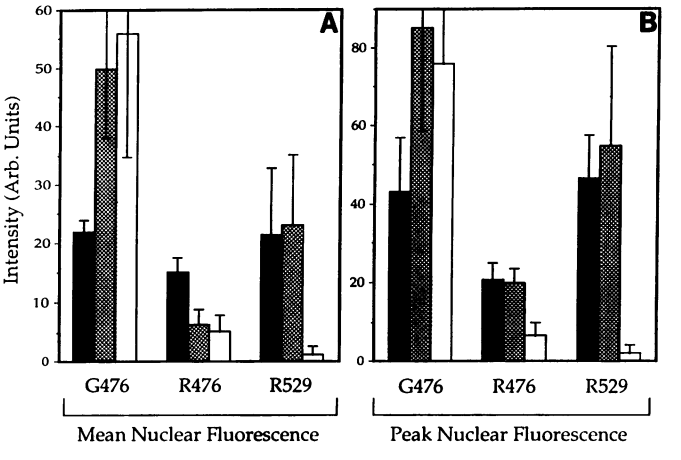

Figure 3. Comparison of specific and non-specific energy transfer in the nucleus of mouse 3T3 cells. Cells were injected with either −PT-F/+PD-R annealed at a 2:1 molar ratio (solid), −PT-F and Actin-Rho annealed at a 2:1 molar ratio (stippled), or −PT-F alone (white). **A** shows the mean nucleoplasmic intensity values of an 8 pixel wide line drawn across nucleus while avoiding any punctate regions. **B** shows the peak intensity values of a 4 pixel wide line drawn through the brightest punctate object within the nucleus. All values were background subtracted; the backgrounds were 13−14 for the G476 channel and 11−12 for the R476 and R529 channels. The number of cells injected with −PT-F, −PT-F/+PD-R and −PT-F/Actin-Rho ODN were respectively 5, 12 and 10.

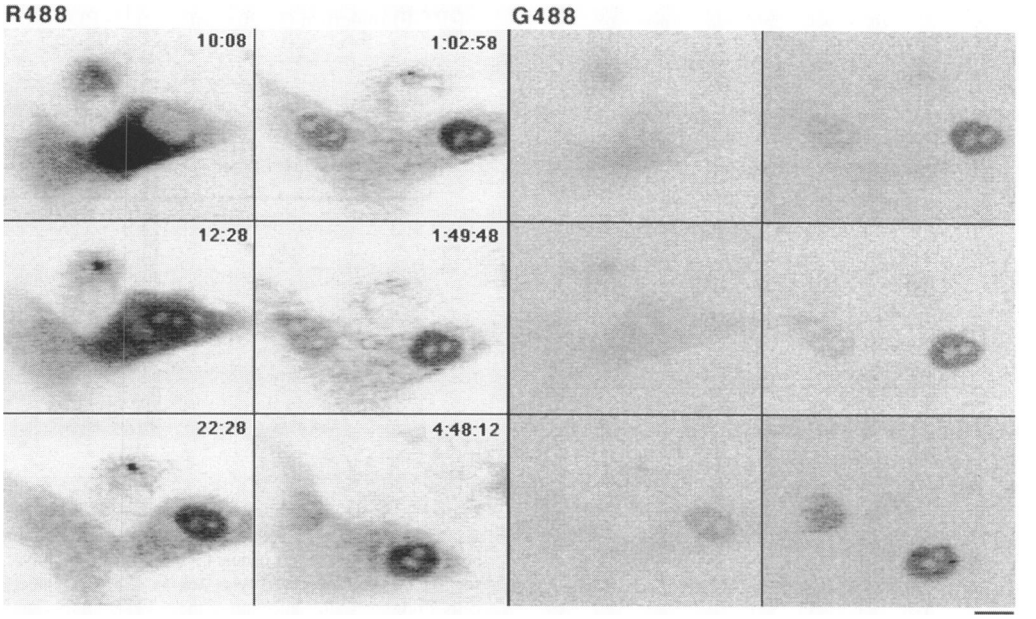

Figure 4. Dissolution of a pre-formed −PT-F/+PD-R hybrid complex in BSC-1 cells. A 1:2 molar ratio of the −PT-F/+PD-R ODNs was mixed, denatured and cooled prior to injection into the cytoplasm of BSC-1 cells. The left panels with indicated elapsed times correspond to the red emission channel (605−665 nm) excited by the 488 nm laser line. Elapsed times are relative to the start of injecting a line of cells. For the cell shown, the first elapsed time after injection is about 1 minute. The right panels are the fluorescein (500−540 nm) emission images. Similar results are obtained with 3T3 cells (data not shown). The bar represents 10 μm.

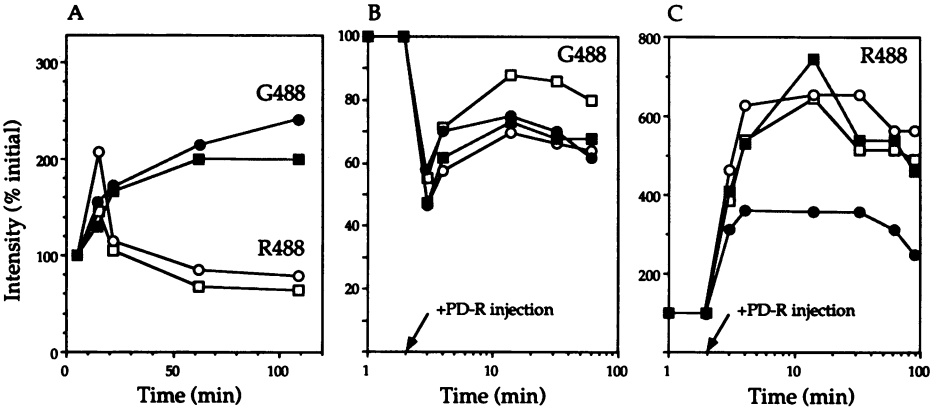

Figure 5. Profile plots of fluorescence values of BSC-1 cells injected with pre-formed −PT-F /+PD-R hybrid complex (panel **A**) and serial injections (panels **B** and **C**). In panel A, the sharp spike of rhodamine emission corresponds to the filling of the nucleus, i.e. the first time point was taken before nuclear accumulation of the oligonucleotides. Mean (squares) and maximum (circles) values are represented for both fluorescein (closed symbols) and rhodamine emissions (open symbols), respectively. In panels B and C, images were taken for four different cells, after injection of the +PD-R oligonucleotide which was injected 20 min after −PT-F injection. Panel B shows the fluorescein emission pattern and panel C shows the rhodamine signal.

Characterization of the confocal module's spectral sensitivity. We optimized the use of the confocal laser scanning microscope for the detection of fluorescence energy transfer by selecting the dichroic mirror and band-pass filter combinations to ensure specific detection of donor quenching and energy transfer. Crossover of fluorescein emission in the red chanel (605−665 nm) with the 474/476 nm (or 488 nm) lines was 14% the intensity found in the green channel (500−540 nm, not shown). Most importantly, excitation of the +PD-R ODN with the 474/476 nm laser lines resulted in very little red emission (12% of the red emission from excitation at 529 nm, not shown). In some experiments, the 488 nm line was used to monitor only fluorescein quenching by the +PD-R ODN. The 474/476 nm lines enabled monitoring both fluorescein quenching and energy transfer to the rhodamine. As expected, intense red emission was observed when the −PT-F/+PD-R hybrid was illuminated with either the 476 nm or 529 nm line (not shown).

Controls for non-hybridization mediated FRET in cells. FRET depends upon the proximity between the donor and acceptor fluorophore. Since ODNs accumulate in distinct (12, 13) and possibly specific sites in the nucleus (14, 15), FRET could occur because fluorescein and rhodamine ODNs bind to adjacent sites within the energy transfer distance. To examine for this

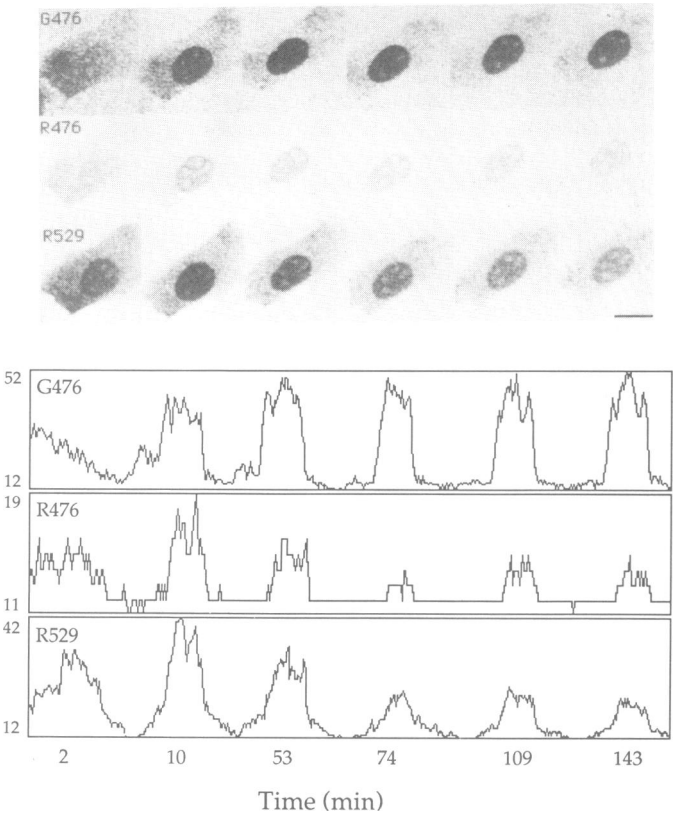

Figure 6. Top—Dissolution of a pre-formed −PT-F/+PD-R hybrid complex in mouse 3T3 cells excited by the 474/476 nm laser lines. A −PT-F/+PD-R hybrid complex was formed at a 1:1 molar ratio as described above and injected into 3T3 cells. The green fluorescein emission (G476, 500−540 nm) and red rhodamine emissions are shown. (R476): 605−665 nm emission with λex = 474/476, and (R529): 605−665 nm emission with λex = 529 line. Bottom—Profile plots through the cells shown. Background fluorescence values are shown at the bottom of the ordinate. The bar represents 10 μm.

possibility, we microinjected the −PT-F with a non-complementary rhodamine 16-mer ODN (Actin-Rho) and measured the fluorescence behavior in single cells. For the specific ODN pair, the mean nuclear green fluorescence was less than the −PT-F alone or the −PT-F/Actin-Rho pair (Figure 3A). The mean, nuclear red fluorescence excited by the 476 nm line was significantly greater for the specific pair (indicative of FRET) than either the non-specific pair or the −F-PT alone (Figure 3A) even though both the specific and non-specific pairs gave similar red emission when irradiated by the 529 nm line. Both the fluorescein quenching and rhodamine fluorescence increase are consistent with specific hybridization occuring in the nucleus.

In discrete regions, of high nuclear fluorescence (peak nuclear fluorescence), the fluorescein emission signal from the specific pair of ODNs was again less than that in the other two treatments when the 476 nm line was used (Figure 3B). However there was no difference between the emission in the red channel of the specific and non-specific pairs. The rhodamine signal arising from excitation at 529 nm was the same, indicating a similar amount of material was injected in both experiments. The increase in the rhodamine signal when excited at 476 nm, may indicate that FRET, unrelated to hybrid formation, may occur. This could be due to the binding to ODNs to structures that position the fluorophores within the energy transfer distance.

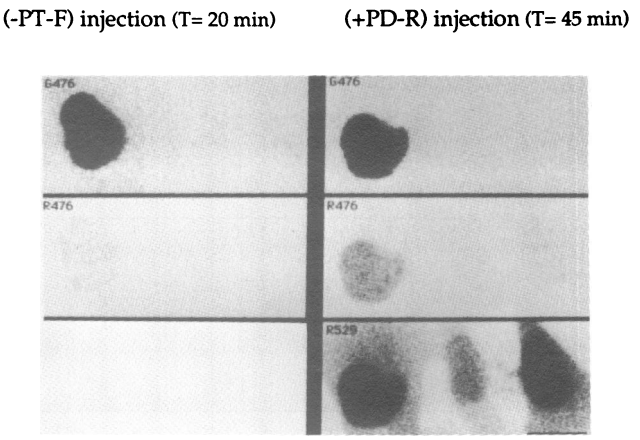

Figure 7. Serial injection of −PT-F and +PD-R ODNs. (A) The −PT-F ODN was injected into 3T3 cells and incubated for 20 minutes to allow the nuclear accumulation. In the left panels (−PT-F injection only), very little red emission for −PT-F was observed with λex = 474/476. Panels on the right show the cells 25 minutes after injection of the +PD-R ODN. The −PT-F was not initially injected in two neighboring cells. Note that only the double injected cell has a R476 signal. The labeling of fluorescein and rhodamine emissions with the appropriate excitation laser lines are as described in previous legends. The bar represents 10 μm.

Increased magnification (84× − 120 ×) of experiments that involved serial injections of the ODNs (*vide infra*) revealed heterogeneous fluorescent regions within the nucleus. Punctate regions were observed in the red emission channel with λex = 474/476 nm, (data not shown). These were absent from both the red emission channel from 529 nm excitation and the green emission channel from λex = 474/476 nm. The nature and stability of these unique structures are the focus of further studies.

Dissolution of pre-formed ODN hybrids. Microinjection of the −PT-F/+PD-R hybrid into the cytoplasm of living 3T3 or BSC-1 cells enabled us to determine both the localization and decay rate of the hybrid. To obtain the maximal donor quenching, a 1:2 molar ratio (10 A units/ml of −PT-F and 20 A units/ml of +PD-R in the injection needle) of the denatured and reannealed −PT-F/+PD-R hybrid was injected. As found previously (12), nuclear accumulation of the rhodamine (605−665 nm) emission rapidly occured (Figure 4). At the 1:2 molar ratio of −PT-F/+PD-R, complete quenching of the fluorescein signal was observed at early times. The intensity of fluorescein fluorescence slowly increased within the nucleus. A collection of experiments performed with the 488 nm laser line confirmed transient quenching of −PT-F in the nucleus (Figure 5).

When both fluorescence quenching and exchange (at a 1:1 molar ratio with λex = 474/476 nm) was monitored (Figure 6), the fluorescence signal started low (2 minutes) and increased with time (10 to 53 minutes). The red signal (with λex = 529 nm or λex = 474/476 nm lines) decreased with time from 10 to 53 minutes (Figure 6). We interpret these findings to result from the loss of fluorescein quenching (i.e., increase in FITC emission) due to loss of energy exchange upon disruption of the hybrid. The non-uniform distribution of ODNs within the nucleus described above, and (12), complicates the quantitation of energy transfer. Nonetheless, the loss of energy transfer over time can be used to estimate the half-life of the duplex. From examination

of over 100 cells in 8 experiments, the half-life of the hybrid (−PT-F/+PD-R) within injected cells was about 15 minutes.

Formation of hybrids in living cells can be determined by serial microinjection. To determine whether the hybridization of the −PT-F and +PD-R ODNs could be detected within living cells, we performed serial injections, Figure 7. The −PT-F ODN was injected into the cytoplasm of a line of selected cells, and allowed to accumulate within the nucleus over a 20 minute period. Cells injected only with −PT-F showed a gradual decrease in overall fluorescence concomitant with nuclear accumulation (data not shown, 12). Subsequently, several of the same cells were injected with the +PD-R ODN. Neighboring cells, uninjected with the −PT-F ODN, were injected with the +PD-R ODN alone. FRET was demonstrated in the nucleus by a transient loss of green fluorescence emission (500−540 nm with λex = 474/476 nm) and an increase in red fluorescence emission (605−665 nm with λex = 474/476 nm). Note that in a neighboring cell, injected with the +PD-R ODN alone, only minimal rhodamine emission with λex = 474/476 nm was found (Figure 7). In other serial injection experiments, when the +PT-R ODN was injected only 2−5 min after λPT-F injection, or when non-hybrid mixtures of −PT-F and +PD-R at 1:2 ratios were injected, transient FRET in the cytoplasm was revealed by quenching of the -PT-F emission and an increase in the red emission (λex=474/476 or 488 nm, not shown). These results suggest that hybrid complexes can form in the cytoplasm prior to nuclear accumulation.

In time course studies of serial injections, a transient reduction of the mean −PT-F ODN green emission coincided with a rapid rise in red emission from the +PD-R ODN which likely resulted from inefficient hybridization of the ~ 1:1 molar ratio (not shown). Thus, *in situ* hybridization is likely complicated by cellular factors including nucleases that can rapidly degrade the phosphodiester ODN, as suggested by the rapid loss of rhodamine emission. Additionally, cellular proteins may bind ssDNA and prevent hybridization while other proteins may disrupt double-stranded nucleic acid complexes (16).

DISCUSSION

We have shown specific hybridization between complementary ODNs bearing donor and acceptor fluorophores by a number of criteria including gel retardation and fluorescence resonance energy transfer in solution. The stability of the complex was characterized by nuclease digestion, competition by unlabeled ODN or nonspecific single-stranded DNA. Two results of the spectrofluorimetry studies stimulated us to extend these studies to living cells. First, the energy transfer *in vitro* was relatively efficient at a 1:1 molar ratio of −PT-F/+PD-R, a 74% quenching of the fluorescein was correlated with a 53% increase in the rhodamine emission. Second, in characterizing the annealing conditions, we found nearly complete hybridization in physiological salts at 37°C.

Examination of hybrid behavior in living cells was explored by microinjection of pre-formed hybrids into cells and by separate, serial injection of the donor (−PT-F) and acceptor (+PD-R) ODNs. The former experiments allowed us to estimate the dissolution rate of the complex. Since the fate of ODNs that enter the cytoplasm is the nucleus (12,13), monitoring dissolution was potentially complicated by the redistribution of hybrids within cellular compartments. It is possible that proteins or cytoplasmic nucleases could disrupt the complex or degrade the +PD-R ODN before nuclear accumulation. This is unlikely since (i) the bulk of the rhodamine signal accumulated into the nucleus at similar rates as free +PD-R (12), (ii) the previously quenched fluorescein signal reappeared in the nucleus with the same time course as the diminution of the rhodamine signal and (iii) fluorescent mononucleotides diffuse from cells into medium within about 10 minutes (12). Thus, complex dissolution may result from hydrolysis of the rhodamine moiety, or unfavorable nuclear salt concentrations, or binding to nuclear proteins. The limited aqueous space in the nucleus might predispose such interactions (17). To determine if such conditions and the vast complexity of genome sequences and nuclear RNA could prevent the formation of complexes, we performed serial injection experiments.

Both the formation and disruption of hybrid complexes were revealed by serial injection experiments. The transient quenching of the donor fluorophore was temporally matched by the rise and fall of the nuclear acceptor rhodamine emission. Strikingly, the rate of hybrid dissolution was similar to the rate of disruption of pre-formed complexes injected into cells. Together, these results suggest that a phosphodiester ODN can hybridize to at least a phosphorothioate ODN, even if only for a short period within cells.

ODNs appear to inhibit gene expression in a sequence-specific manner, but the problems of nonspecific effects on cells, ODN stability and inefficient delivery remain unsolved (for a review, 18). The diverse effects of ODNs may be related to their distribution and degradation within cells. Our results indicating a short intracellular life-time for phosphodiesters may help to explain the diverse range of effects of previous studies employing phosphodiesters (19−24). Continuing these studies with a variety of targets, chemical linkages and conditions should improve our understanding of the parameters affecting efficient and long-lived hybrid complexes within cells. The ability to detect FRET from hybridized ODNs in cells also opens the way to monitor the binding of fluorescent antisense ODNs to specific RNA. In fact, we have detected FRET between a 5′ fluorescein labeled anti-actin ODN and a 3′ rhodamine labeled anti-actin ODN that bind to adjacent locations on actin mRNA (25). This technique may permit the optical tracking of various RNA molecules inside living cells and would augment immunohistochemical techniques (26) for the detection of RNA trafficking in cells.

ACKNOWLEDGEMENTS

We are grateful to helpful comments and suggestions from R.Stull in the selection of ODN sequences and to Dr A.Verkman and S.Bickness for the use of the time resolved fluorescence spectrometer. This work has been supported by grants from 'La Fondation pour la Recherche Thérapeutique' (SS), NIH GM30163 (FCS) and NIH AI30880 (DJC).

REFERENCES

1. Zamecnik, P.C. and Stephenson, M.L. (1978) *Proc. Natl. Acad. Sci. USA*, **75**, 280−284.
2. Hélène, C. and Toulmé, J.J. (1990) *Biochim. Biophys. Acta*, **1049**, 99−125.
3. Léonetti, J.P., Clarenc, J.P. Degols, G., Mechti, N. and Lebleu, B. (1993) *Prog. Nucl. Ac. Res. Mol. Biol.*, **44**, 143−166.
4. Chiang, M.Y., Chan, H., Zounes, M.A., Freier S.M., Lima, W.F. and Bennett C.F. (1991) *J. Biol. Chem.* **266**, 27, 18162−18171.
5. Simons, M., Edelman, E.R., DeKeyser, J.L., Langer, R. and Rosenberg, R.D. (1992) *Nature*, **359**, 67−70.

6. Woolf, T.M., Melton, D.A. and Jennings, C.G.B. (1992) *Proc. Natl. Acad. Sci. USA*, **89,** 7305–7309.
7. Cardullo, R.A., Agrawal, S., Flores, C., Zamecnik, P.C. and Wolf, D.E. (1988) *Proc. Natl. Acad. Sci. USA* , **85,** 8790–8794.
8. Morrison, L.E., Halder, T.C. and Stols, L.M. (1989) *Analytical Biochem.*, **183,** 231–244.
9. Clegg, R.M., Murchie, A.L.H., Zechel, A. and Lilley, D.M. (1993) *Proc. Natl. Acad. Sci. USA*, **90,** 2994–2998.
10. Zon, G. and Geiser T.G. (1991) *Anti-Cancer Drug Design,* **6,** 539–568.
11. Roe, J.N., Szoka, F.C. and Verkman, A.S. (1989) *Biophys. Chem.*, **33,** 295–302.
12. Chin, D.J., Green, G.A., Zon, G., Szoka Jr, F.C. and Straubinger, R.M. (1990) *The New Biologist,* **2,** 1091–1100.
13. Léonetti, J.P., Mechti, N., Degols, G., Gagnor, C. and Lebleu, B. (1991) *Proc. Natl. Acad. Sci. USA*, **88**, 2702–2706.
14. Geselowitz, D.A. and Neckers, L.M. (1992) *Antisense Res. Develop.*, **2,** 17–25.
15. Clarenc, J.P., Lebleu, B. and Léonetti, J.P., L. (1993) *J. Biol. Chem.*, **268,** 8, 5600–5604.
16. Wagner, R.W. and Nishikura K. (1988) *Mol. Cell Biol.*, **8,** 2, 770–777.
17. Paddy, M.R., Belmont, A.S., Saumweber, H., Agard, D.A. and Sedat, J.W. (1990) *Cell,* **62, 1,** 89–106.
18. Cohen, J.S. (1992) *Trends in Biotech.*, **10,** 3, 87–91.
19. Agrawal, S., Ikeuchi, T., Sun, D., Sarin, P.S., Konopka, A., Maizel, J. and Zamecnik, P.C. (1989) *Proc. Natl. Acad. Sci. USA*, **86,** 7790–7794.
20. Burch, R.M. and Mahan, L.C. (1991) *J. Clin. Invest.*, **88,** 1190–1196.
21. Goodchild, J., Agrawal, S., Civeira, M.P., Sarin, P.S., Sun, D. and Zamecnik, P.C. (1988) *Proc. Natl. Acad. Sci. USA*, **85,** 5507–5511.
22. Letsinger, R.L., Zhang, G.R., Sun, D.K., Ikeuchi, T. and Sarin, P.S. (1989) *Proc. Natl. Acad. Sci. USA*, **86,** 6553–6556.
23. Matsukura, M., Shinozuka, K., Zon, G., Mitsuya, H., Reitz, M., Cohen, J.S. and Broder, S. (1987) *Proc. Natl. Acad. Sci. USA,* **84,** 7706–7710.
24. Smith, C.C., Aurelian, L., Reddy, M.P., Miller, P.S. and Ts'o, P.O. (1986) *Proc. Natl. Acad. Sci. USA*, **83,** 2787–2791.
25. Sixou, S., Szoka Jr , F.C., Zon, F.C. and Chin, D.J., (unpublished)
26. Wansink, D.G., Schul, W., van der Kraan, I., van Driel, R. and de Jong, L. (1993) *J. Cell Biol.*, **122,** 2, 283–293.